Theor Appl Climatol (2018) 133:681–695
DOI 10.1007/s00704-017-2196-4

ORIGINAL PAPER

The impact of heat waves on surface urban heat island and local economy in Cluj-Napoca city, Romania

Ioana Herbel[1] · Adina-Eliza Croitoru[2] · Adina Viorica Rus[3] · Cristina Florina Roşca[1] · Gabriela Victoria Harpa[1] · Antoniu-Flavius Ciupertea[1] · Ionuț Rus[1]

Received: 27 November 2016 / Accepted: 7 June 2017 / Published online: 12 July 2017
© Springer-Verlag GmbH Austria 2017

Abstract The association between heat waves and the urban heat island effect can increase the impact on environment and society inducing biophysical hazards. Heat stress and their associated public health problems are among the most frequent. This paper explores the heat waves impact on surface urban heat island and on the local economy loss during three heat periods in Cluj-Napoca city in the summer of 2015. The heat wave events were identified based on daily maximum temperature, and they were divided into three classes considering the intensity threshold: moderate heat waves (daily maximum temperature exceeding the 90th percentile), severe heat waves (daily maximum temperature over the 95th percentile), and extremely severe heat waves (daily maximum temperature exceeding the 98th percentile). The minimum length of an event was of minimum three consecutive days. The surface urban heat island was detected based on land surface temperature derived from Landsat 8 thermal infrared data, while the economic impact was estimated based on data on work force structure and work productivity in Cluj-Napoca derived from the data released by Eurostat, National Bank of Romania, and National Institute of Statistics. The results indicate that the intensity and spatial extension of surface urban heat island could be governed by the magnitude of the heat wave event, but due to the low number of satellite images available, we should consider this information only as preliminary results. Thermal infrared remote sensing has proven to be a very efficient method to study surface urban heat island, due to the fact that the synoptic conditions associated with heat wave events usually favor cloud free image. The resolution of the OLI_TIRS sensor provided good results for a mid-extension city, but the low revisiting time is still a drawback. The potential economic loss was calculated for the working days during heat waves and the estimated loss reached more than 2.5 mil. EUR for each heat wave day at city scale, cumulating more than 38 mil. EUR for the three cases considered.

✉ Adina-Eliza Croitoru
croitoru@geografie.ubbcluj.ro; adina04@yahoo.com

[1] Faculty of Geography, Babeş-Bolyai University, 5-7, Clinicilor Street, 400006 Cluj-Napoca, Romania

[2] Faculty of Geography, Department of Physical and Technical Geography, Babeş-Bolyai University, 5-7, Clinicilor Street, 400006 Cluj-Napoca, Romania

[3] Faculty of Economics and Business Administration, Department of Political Economy, Babeş-Bolyai University, 58-60, Teodor Mihali Street, 400591 Cluj-Napoca, Romania

1 Introduction

Heat waves (HWs) usually occur in synoptic conditions with pronounced slow air mass development and movement (Unger et al. 2014). During the summer, they can be particularly intense in urban areas, where the geometry and thermal properties of surfaces, correlated with high levels of anthropogenic heat, alter the energy balance as compared to nearby rural areas (Laaidi et al. 2012). The association of HWs with the urban heat island (UHI) effect can increase the impact on environment and society inducing a great variety of biophysical hazards. Among them, heat stress, air pollution, and associated public health problems are the most frequent (Zhou and Shepherd 2010). The urban and rural mortality rates during HWs were investigated by Gabriel and Endlicher (2011) for the cases of Berlin and Brandenburg, concluding that during the two main heat events that occurred between 1990 and

2006, the highest mortality rates were recorded in the most densely built-up districts in the city of Berlin. Such findings and the large number of fatalities from intense HWs, such as the one recorded in 2003 in Europe that resulted in 70,000 heat-related deaths (Robine et al. 2008), demand sustained research efforts that should be focused on the behavior of UHI during HW periods and on the development of site-specific mitigation strategies, including early warning systems for HWs (Ćurić 2012; Radinovic and Curic 2013).

The UHI is well documented for many cities worldwide. By 2011, the magnitude and spatial extension of the phenomenon had been explored in more than 200 cities and towns (Stewart 2011). Some of those studies focused on the characteristics of the UHI during heat events (Kawashima et al. 2000; Cheval et al. 2009; Basara et al. 2010; Tan et al. 2010; Zhou and Shepherd 2010; Dousset et al. 2011; Laaidi et al. 2012; Apostol et al. 2012; Li and Bou-Zeid 2013; Hu et al. 2015; Icaza et al. 2016; Ward et al. 2016). HWs induced by the persistence of high-pressure anticyclones are usually associated with low wind speed and clear sky, conditions that are known to favor the formation of UHI. The reduced advective cooling generated by colder air from the surrounding rural areas in such conditions can lead to a stronger atmospheric urban heat island (AUHI) effect (Li and Bou-Zeid 2013; Bottyan et al. 2005; Hu and Jia 2009). A thorough understanding of surface urban heat islands (SUHIs) and HWs interaction is still not possible yet due to lack of sufficient research quality data, but some authors have surmised that the heat island effect is responsible for modulating environmental conditions during HW periods (Basara et al. 2010). Since UHIs are characterized by higher temperature values, they can potentially increase the magnitude and duration of heat events in the urban environment (Tan et al. 2010; Dousset et al. 2011). Such an assumption is in agreement with the findings reported by Campetella and Rusticucci (1998), who analyzed an extreme HW event over Argentina and pointed out that it was more intense during the night in Buenos Aires compared to rural areas, due to the absence of the nocturnal ventilation effect. On the other hand, there is strong evidence that HWs lead to a pronounced amplification of nighttime urban-rural temperature difference. Research focused on the AUHI-HW interaction in two North-American cities revealed that both observations and simulations indicate that the heat island is amplified under HW conditions (Li and Bou-Zeid 2013; Hu et al. 2015). The same conclusion was drawn by other authors studying different cities in Europe, concerning both AUHI (Founda et al. 2015) and SUHI (Dousset et al. 2011; Icaza et al. 2016; Ward et al. 2016). Thus, there are good reasons supporting the hypothesis of a mutual reinforcing relationship between HWs and UHIs.

Some of the studies were performed using low spatial resolution sensors due to their high revisiting time, which allows a better synchronicity with in situ data. Gallo et al. (1993), working with Advanced Very High Resolution Radiometer (AVHRR), concluded that the derived surface temperature was minimally related to the observed urban-rural differences. On the other hand, Prihodko and Goward (1997) used data from the same platform, obtaining a coefficient of 0.93 between ambient and surface temperatures. Relatively strong correlations between these two variables were also identified using helicopter based remote sensing (Stoll and Brazel 1992), airborne thermal radiometry (Ben-Dor and Saaroni 1997; Unger et al. 2010) and thermal infrared (TIR) satellite data, provided by platforms such as Landsat (Kawashima et al. 2000) and Advanced Spaceborne Thermal Emission and Reflection Radiometer (ASTER) (Nichol et al. 2009). Based on this evidence, we can infer that, although the relationship is always the same in reality, technically, the retrieving may depend on the spatial resolution of the sensor which seems to be a key factor that influences the strength of correlation between the two types of temperature. The biased spatial sampling of surface temperature by remote sensors can also reduce the significance of the relationship because the temperature of a pixel is obtained by spatial averaging a complex surface temperature. This value may be disproportionately weighted in favor of one surface type (Roth et al. 1989), and the effect is more pronounced at lower spatial resolutions and in heterogeneous surfaces, like the urban environment. In such a complex area, a micro-advection from adjacent land is supposed to reduce the level of correlation between air and surfaces temperatures (Stoll and Brazel 1992; Unger et al. 2010).

In terms of impact of such events, many studies conducted in different regions of the world focused on the socio-economic impact of HWs. Some of them (Parsons 2009; Costa et al. 2016; Pogacar et al. 2016) concluded that for sedentary and light activities, it is necessary to cool offices and homes to a temperature lower than 25 °C for thermal comfort, resulting in a substantial increase of energy consumption, while for outdoor activities, special time restriction should be required. A recent study of the economic effects of the HWs conducted in Australia (Zander et al. 2015) estimated a total cost from lost productivity and absenteeism of minimum US$6.2 bn per year, generated by an average loss due to reduced productivity of US$932 per person per year, as a result of 10 days a year spent under severe heat stress. This amount not only lacks to consider the volunteer and caregiver activities but was also calculated based on the Australian economy, which is strongly adapted to high temperature conditions and where the employers already do a lot to alleviate the temperature stress. In Europe and especially in Romania, the cost of a severe HW, though less frequent than in Australia, can be expected to be significantly higher due to the lack of information released to population, since all the warnings are issued considering temperature values recorded by weather stations and not those registered in the city area (under the influence of UHIs).

For the Romania's territory, few studies on UHI and relationship between UHI and HWs have been conducted so far. Few of them focused on the geometry and intensity of SUHI by using land surface temperature (LST) derived from Moderate-Resolution Imaging Spectroradiometer (MODIS), such as those performed for Bucharest city in summer time or under HW conditions (Cheval and Dumitrescu 2009; Cheval and Dumitrescu 2015; Cheval et al. 2009). The studies showed that the nocturnal changes refer mainly to the magnitude and the limits of the UHI, but not the shape, while the diurnal UHI patterns were modified by the extreme temperatures of the HWs. Good correlations were found between LST and air temperature data from three meteorological stations. Another study investigated the intensity of AUHI in Iasi municipality during a 10-day HW event in July 2011 (Apostol et al. 2012). The maximum AUHI intensity reported for the daytime was about 8.0 °C. Only one study considered the general classes of socio-economic impact of HWs in Bucharest city, but the impact was not converted into economic loss (Croitoru et al. 2014).

Therefore, the main objectives of this paper are to identify the spatial patterns of the SUHI in Cluj-Napoca city under HW conditions based on Landsat 8 derived LST, as well as to briefly estimate the socio-economic impact of HWs for those events occurred in Cluj-Napoca city in the summer of 2015.

2 Materials and methods

2.1 Study area

The present study is focused on Cluj-Napoca city area, located in the northwestern part of Romania (Fig. 1). It is the second most populated city after the capital of the country (Bucharest city), with a stable population of more than 320,000 inhabitants. Among them, 90,000 are working people. As one of the most important academic and cultural centers of the country, it also attracts a floating population of students, which is around 70,000 people every year. Characterized by a continental climate with western oceanic influences, the city is located in a hilly region, near the Apuseni Mountains (part of the Western Carpathians), along Someșul Mic River valley. The altitude ranges mainly between 300 and 400 m above the sea level, and the topography and geology are restrictive factors for horizontal urban expansion since the city is surrounded in its western, northern, and southern parts by unstable hills up to 920 m height, frequently affected by landslides. The geometry and the landscape of the city (dominated by asphalt and concrete buildings) are mainly the result of the massive urbanization process launched by the communist regime in the 1960s, when high-density blocks of flats were built to sustain the rural exodus. The newly built neighborhoods were appended to the rather compact historical city center with a relatively low height regime. Since the UHI intensity implies a temperature difference between the urban area and the nearby rural

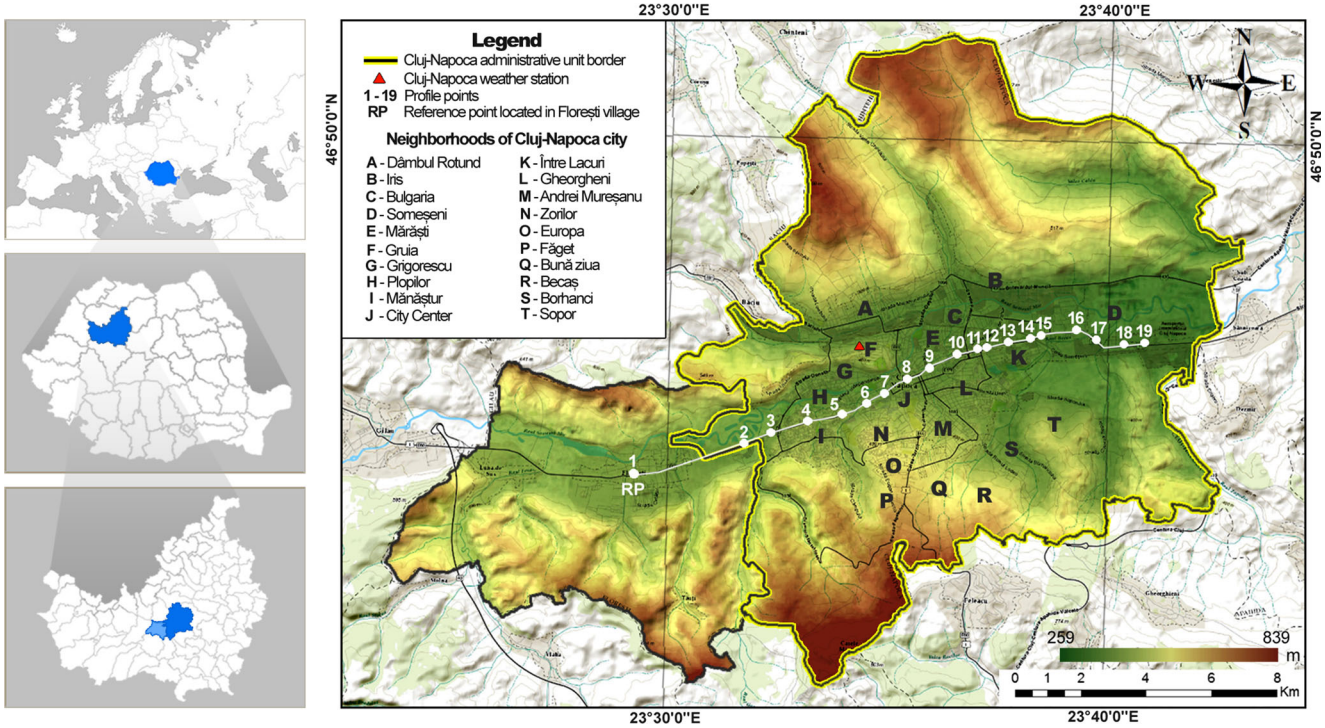

Fig. 1 Study area and the transect over the city for LST analysis

area, one adjacent commune (Floreşti) was also included in our analysis for further data processing (Fig. 1).

2.2 Data used

2.2.1 HW definition and near surface air temperature data

The HW events have been assessed based on the daily maximum air temperature (TX) data recorded by Cluj-Napoca weather station (WMO code 15120), located in the city area. The non-blend data set for 1981–2009 was freely downloaded from ECA&D project database (Klein Tank et al. 2002) and reconstructed based on raw SYNOP messages available on www.meteomanz.com for 2010–2015 (Meteomanz 2016). The surface conditions recorded by Cluj-Napoca weather station used to estimate the parameters for the atmospheric corrections of LST were freely downloaded from *Reliable prognosis* database (Reliable prognosis 2016), freely available at http://rp5.ro (Table 1).

For a general analysis of LST derived from satellite data along the city, we selected a number of 19 sample points (point 1 is the reference point, RP) on a representative transect, unaltered by altitude. Crossing from west to east on a distance of about 20 km, it followed the main route axis of the city (Fig. 1).

The deviation values of the sample points against the reference point (RP or point 1) were selected for further analysis.

2.2.2 Synoptic analysis data

The synoptic analysis was performed based on reanalysis synoptic maps of sea level pressure and geopotential at 500 hPa level, freely downloaded from Karlsruhe Weather Center e-archive (Wetterzentrale 2016), freely available at www.wetterzentrale.de. Because the satellite images were captured a few minutes after 9:00 UTC (around mid-day, Romanian Summer Time (RST)), for synoptic analysis, we used two maps for each of the three case studies. In order to have a detailed analysis of the synoptic conditions, we considered necessary to cover the interval before and after the moment of the image capture, so we decided to choose the maps valid for 00:00 and 12:00 UTC.

2.2.3 Satellite image data acquisition

In order to analyze SUHI under HW conditions, first we selected 15 satellite images available over a 15-year period (2001–2015) for summer season (June-August). For further analysis, we retained only three of them, captured in the summer of 2015 (July 7, July 23, and August 8), as they were the only ones recorded during HW events. In two other situations (July 2002 and July 2007), the intensity threshold (the value of a specified percentile) for an HW event was exceeded, but the duration threshold (at least three consecutive days) was not reached (Table 2).

In order to detect SUHI during HWs, for this study, we employed Landsat 8 satellite scenes freely downloaded from the United States Geological Survey database (USGS 2016) freely available at https://earthexplorer.usgs.gov/. The satellite images were used for computing the LST. They were acquired by the Operational Land Imager Thermal Infrared Sensors (OLI_TIRS) on the abovementioned dates. The scene center time for each image was 09:14 UTC (12:14, RST). The cloud cover value for each of the chosen scene was different from one image to another, with no more than 2.65% cloudiness for each image, but the study area was cloud free for each of the case studies considered. Due to the influence of stray light, the Landsat project team recommends users to refrain from using band 11 in split-window surface temperature algorithms. Therefore, the second band was excluded from the study because it is more contaminated by the thermal energy from outside the normal field of view and can increase the reported temperature by up to 10 K (Department of the Interior U.S. Geological Survey 2016). Thus, for LST retrieval, only band 10 was retained. With a (resampled) spatial resolution of 30 m, it covers the range between 10.6 and 11.19 μm from the electromagnetic spectrum, an interval located in a lower atmospheric absorption region than the one covered by band 11 (Jiménez-Muñoz et al. 2014). In addition, the red and near-infrared bands of the same scenes were used to compute the Normalized Difference Vegetation Index (NDVI).

2.2.4 Data for economic impact estimation

During our study, we found it very difficult to aggregate economic data on the cost at local level, as the lack of readily

Table 1 Weather conditions and resulted correction parameters

tbcolw55ptDate	Time of satellite image capture (UTC)	Time of weather observations (UTC)	Air temperature (°C)	SLP (hPa)	Relative humidity (%)	Atmospheric transmission (τ)	Upwelling long wave radiance (L_u)	Down welling long wave radiance (L_d)
July 7, 2015	09:14:26	9:00	29.5	1018.0	48	0.66	2.89	4.56
July 23, 2015	09:14:33	9:00	29.4	1015.1	57	0.59	3.45	5.33
August 8, 2015	09:14:36	9:00	28.9	1022.7	34	0.88	1.05	1.78

Table 2 Dates of satellite images capture and HW conditions in summer months over the period 2001–2015

Satellite image date	Heat waves type	HW start date	HW final date	*Ta* at the time of satellite image[a] (°C)	TX in the day of satellite image[b] (°C)	TX of the HW[c] (°C)
August 2, 2001	No HW	–	–	24.6	27.2	–
July 4, 2002	No HW	–	–	28.2	34.1	–
June 29, 2003	No HW	–	–	23.8	28.2	–
July 22, 2003	No HW	–	–	25.8	31.4	–
July 23, 2006	No HW	–	–	26.4	29.9	–
July 10, 2007	No HW	–	–	29.1	33.1	–
August 2, 2007	No HW	–	–	21.0	25.2	–
July 06, 2009	No HW	–	–	23.6	26.9	–
July 22, 2009	No HW	–	–	25.3	31.0	–
August 3, 2010	No HW	–	–	26.8	30.6	–
July 26, 2013	No HW	–	–	25.2	28.5	–
August 2, 2013	No HW	–	–	25.8	28.9	–
July 7, 2015	Severe Moderate	July 6 July 6	July 8 July 9	29.5	32.7	33.6
July 23, 2015	Severe Moderate	July 23 July 22	July 25 July 25	29.4	33.3	33.4
August 8, 2015	Extremely severe Severe Extremely severe	August 5 August 4 August 10	August 8 August 16 August 15	28.9	32.6	33.7 35.6 35.6

[a] Air temperature recorded at Cluj-Napoca weather station, at the nearest moment (less than 1 h) to the satellite image capture

[b] Maximum air temperature of the specified day recorded at Cluj-Napoca weather station

[c] The highest maximum daily temperature recorded during the HW event at Cluj-Napoca weather station

available data added to companies' reluctance to measure and communicate exact internal figures. The economical actors, interviewed all over Europe, estimated a productivity at a maximum level of about 70% of regular days during the periods of intense heat (McKinnon et al. 2016). Thus, we used also this value for our area of interest.

In order to estimate the economic impact of HWs, we used data for hourly productivity in Romania for 2015, issued by the National Bank of Romania (2015a, b) and by the European Community through Eurostat platform (European Community 2015, available at: http://ec.europa.eu/eurostat/web/products-datasets/-/tsdec310). The estimation of potential economic loss also considered particular data available for Cluj-Napoca city such as the total numbers of employees (90,000), as well as the official data for work force structure in Cluj-Napoca from the National Institute of Statistics (available at http://www.insse.ro/cms/). We aggregated them for Cluj-Napoca city in order to get the productivity per person per hour.

2.3 Methods

2.3.1 HW identification

The identified HWs consisted of minimum three consecutive days with TX equal to or higher than a specified percentile value of the day over a 30-year reference period (1981–2010): the 90th percentile for moderate HWs, the 95th percentile for severe HWs, and the 98th percentile for extremely severe HWs. For this analysis, we considered three HW events that occurred in the summer of 2015 (Table 2).

2.3.2 NDVI and LST retrieval

The first step was to compute NDVI for each of the three satellite images. The NDVI map was obtained using the red and near-infrared spectral reflectance bands of the satellite scenes. The TIRS sensor of Landsat 8 stores the spectral response of objects from the Earth's surface in the thermal infrared region as digital numbers (DNs) that can be rescaled to top of atmosphere (TOA) radiance using band-specific multiplicative and additive rescaling factors provided in the metadata file. The TOA spectral radiance was obtained by scaling the digital numbers of TIRS-1 (band 10) according to methodology presented in the *Landsat 8 Data User Handbook* (Department of the Interior U.S. Geological Survey 2016).

The emitted signal of the objects is both attenuated and enhanced by the atmosphere (Barsi et al. 2005). The TOA (space reaching) spectral radiance is composed of three different fractions of energy: emitted radiance from the Earth's surface, upwelling radiance from the atmosphere, and downwelling radiance from the sky (Weng et al. 2004). Therefore, the TOA spectral radiance measured by the instrument needed corrections for atmospheric effects. In order to achieve this goal, a web-based atmospheric correction parameter tool developed by Barsi et al. (2005) that uses the MODTRAN radiative transfer code was employed. The mid-latitude summer standard atmosphere for upper atmospheric profile, the Landsat 8 band 10 spectral response curve, and the surface weather conditions were used as input data

for the model. Atmospheric profiles (Fig. 2) and estimated values of the atmospheric transmission, the upwelling radiance, and the downwelling radiance calculated by using the Atmospheric Correction Parameter Calculator application freely available at http://atmcorr.gsfc.nasa.gov (Barsi et al. 2005) are presented in Table 1.

This allowed us to compute the actual surface-leaving radiance as indicated by Yuan and Bauer (2007). The emissivity values were used to scale the blackbody radiance. To identify these values, the NDVI threshold method proposed by Xiong et al. (2012) was used. The vegetation proportion was first calculated with the equation developed by Carlson and Ripley (1997), using extreme NDVI values of 0.05 (as minimum) and 0.70 (as maximum), and the final emissivity raster was obtained according to the method proposed by Sobrino et al. (2004).

The next step was to compute the surface temperature using Planck's law inversion. The method used here was adapted for Landsat 8 based on the equation introduced by Chander and Markham (2003). Since the surface temperature value obtained with this equation is expressed in Kelvin, the final step of the LST retrieval algorithm was to convert LST from Kelvin into Celsius degrees.

2.3.3 LST deviation

The LST deviation of the 18 sample points (numbered from 2 to 19) was calculated for each point as a difference of the surface temperature of each pixel against the surface temperature of the pixel that included RP for all the images considered for this study.

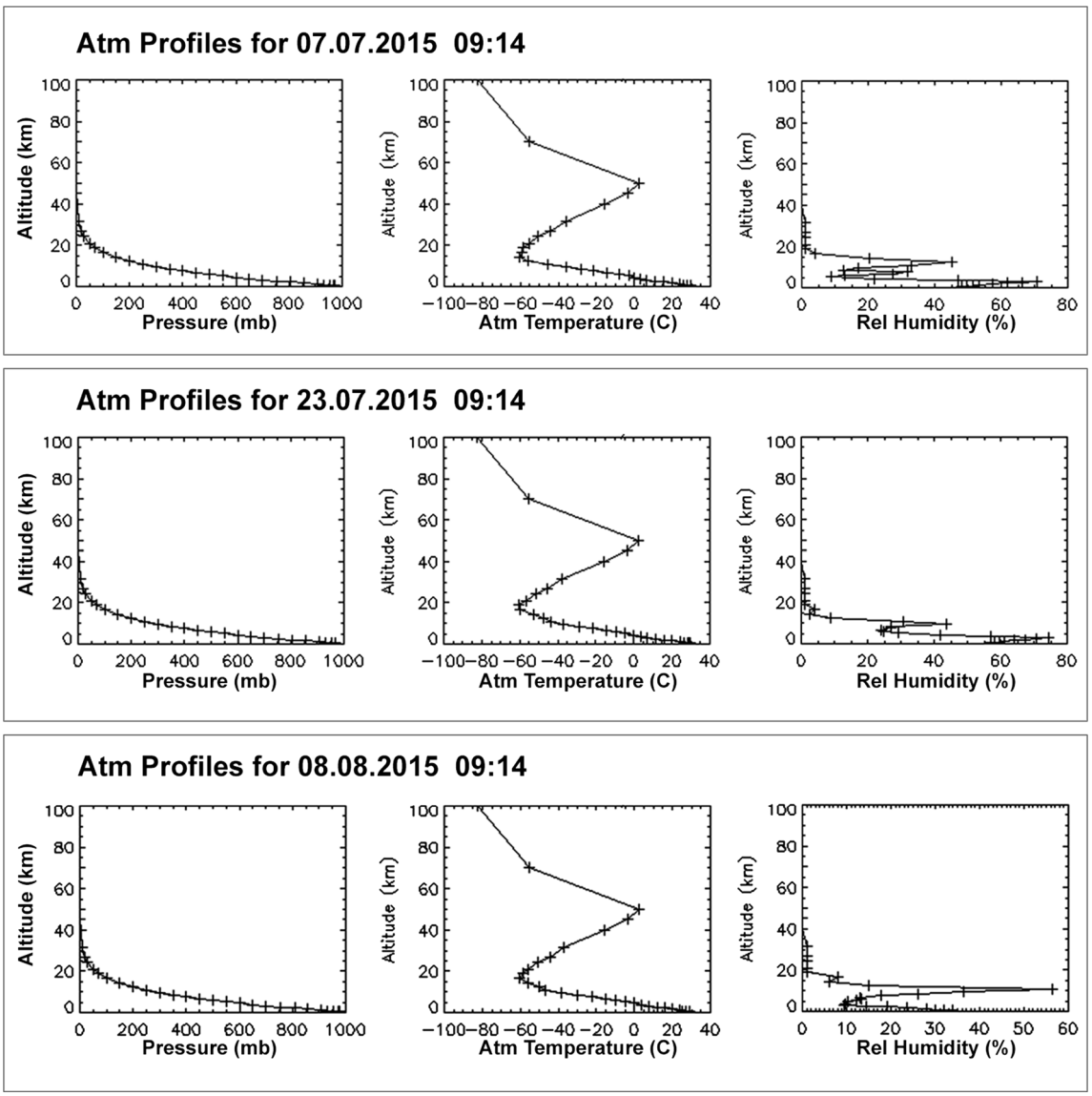

Fig. 2 Atmospheric profiles for July 7, July 23, and August 8, 2015

2.3.4 Mapping

The satellite image data was processed with a model that integrated the operations presented in Sect. 2.3.1. By the end of the geoprocessing workflow, the LST deviation and LST classes from 5 to 5 °C were obtained. All the results were mapped using ArcMap tool included in ArcGIS software v. 10.2.

2.3.5 Estimation of potential economic loss

As presented in Sect. 2.2.4., it was quite difficult to aggregate economic data on the cost at local level. For decreased work productivity due to ambient temperature we used data calculated at European scale, which estimated the work productivity during the periods of intense heat at a maximum level of about 70% of regular days (McKinnon et al. 2016). The other data, such as total numbers of employees and the hourly productivity (P), were calculated for Cluj-Napoca city.

In order to assign a value to the potential economic loss caused by the HWs, we started from the workforce structure and the hourly productivity per sector at national level, based on the official data from the National Institute of Statistics (available at http://www.insse.ro/cms/). The result was a national average productivity of 5.6 EUR/person/h. The number of employees in Cluj-Napoca city was 90,000, in 2015, according to the data from local Work Force Office. We calculated the local workforce distribution. Finally, we applied the national sector productivity data to Cluj-Napoca work force distribution, by using an adjustment reflecting the difference in industrial production structure at local level, and we obtained the estimated hourly productivity of 11.8 EUR/person/h for Cluj-Napoca city.

The economic impact estimation considered data for the total numbers of employees (E) in Cluj-Napoca city of 90,000, and the hourly productivity (P) of 11.8 EUR/person/h. The economic loss (EL) calculation was developed only for working days in the three HWs (detected based on the data recorded by Cluj-Napoca weather station), as in (1).

$$\mathrm{EL} = E \times P \times Lr \times D \quad (1)$$

where

EL—loss productivity (in EUR)
E—total number of employees in Cluj-Napoca in 2015
P—hourly productivity (11.8 EUR/person/h); it was obtained from adjusting the Romanian average of 5.6 EUR/person/h to match the workforce structure in Cluj-Napoca
Lr—productivity loss rate (Lr = 0.3); we used for the productivity loss rate the value estimated at European level by McKinnon et al. (2016)
D—total length of the HW events considered without weekend days, 15 days (given in working hours based on a 8-h working day value)

3 Results and discussions

The occurrence of HWs in Romania in summer is related generally to southern or southwestern advection flows of warm air masses associated with high-pressure systems, originated in North Africa or in Azores (Sfică et al. 2017). Under these circumstances, it is expected to find the highest intensity of UHI in Cluj-Napoca city during summer HWs. From the total number of 15 satellite images available, we analyzed in details those images captured when HW events occurred: July 7, 2015, July 23, 2015, and August 8, 2015. The other ones were used for comparison at the end of this chapter.

3.1 Surface urban heat island extension and intensity on July 7, 2015

The synoptic situation of July 7, 2015 was under the influence of a high ridge originated in Azores High, extended from southwest, over most of Europe, including Romania at 500 hPa level (Fig. 3). At sea level a near normal pressure field (1015–1020 hPa) was dominant. The association of a high-pressure system with a weak advection from southwest (Romania was located under the high ridge axis) generated a severe 3-day HW, starting on July 6, and reaching its highest intensity on the last day, on July 8 (Table 2). For one more day (July 9), the HW continued as moderate HW.

In the second day of the HW event, the satellite image was captured by the OLI_TIRS sensor. At noon, when the satellite passed over the study area, no clouds were recorded at Cluj-Napoca weather station. Therefore, a valid image resulted, and processing the thermal infrared satellite image data allowed the evaluation of the SUHI in Cluj-Napoca in terms of intensity and spatial extension (Fig. 4). For July 7, the LST map of the city and the adjacent commune indicates a strong SUHI, with a mean temperature of 33.1 °C around 12:00 p.m. (RST). The lowest temperature was recorded at Florești water storage reservoir (23.4 °C) and also in regions covered by forests, while the highest temperatures are distributed in the built-up area and over land with low-vegetation coverage. In terms of LST class coverage, the most extended one had temperatures of 30.1–35.0 °C, while more than 28% of the considered area recorded temperatures between 35.1 and 45.0 °C (Table 3).

When compared to the reference point LST, the values in the city were found to be much higher, reaching up to 16 °C difference; the maximum values were specific for large industrial and commercial areas, while the lowest deviations

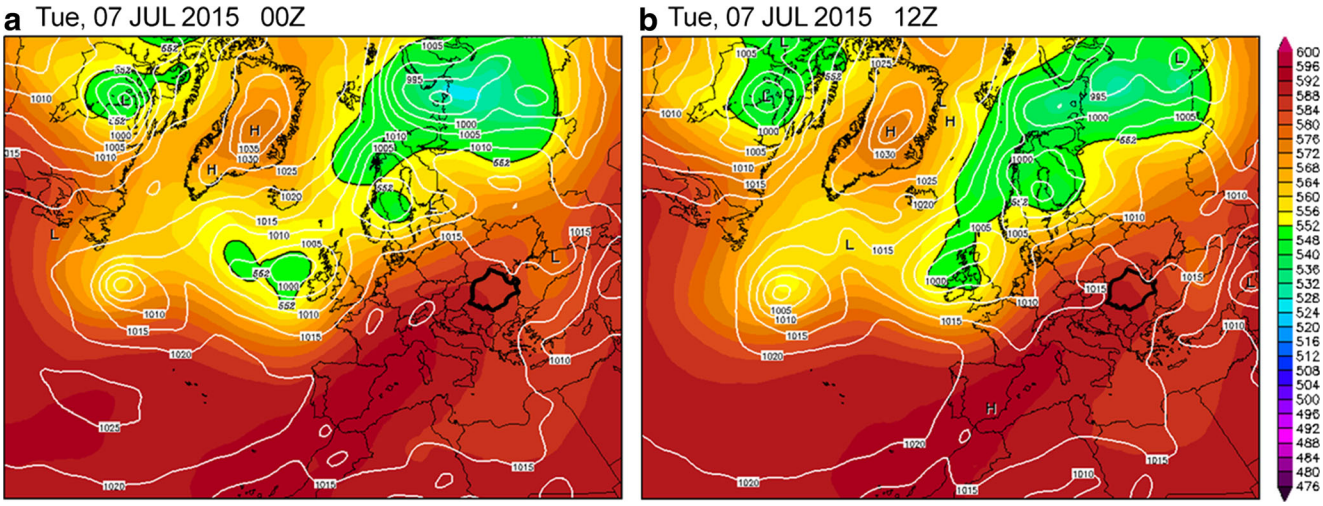

Fig. 3 Synoptic conditions on July 7, 2015 (source www.wetterzentrale.de, modified) at 00:00 UTC (**a**) and at 12:00 UTC (**b**). Romania's territory is emphasized in black thick line

characterized the water bodies (the Someşul Mic River and the storage lake), as well as the green areas.

Inside the city, large hot-spots were identified in the industrial landscape located in the northeastern part of the built-up area, north of the Someşul Mic River, followed by the medieval site of the Old City (with narrow streets, high density of buildings and low albedo rooftops).

Other isolated hot-spots corresponded to industrial and commercial building rooftops. A good example is a hot-spot located in the western part of the city corresponding to a large commercial area, at the border between Cluj-Napoca city and Floreşti village (Fig. 4), where the rooftop and the large asphalt parking in front of it generated temperatures ranging from 45.0 to 55.7 °C. The last mentioned value is the maximum one detected on the LST map generated for July 7. Values higher than 40.0 °C were recorded mainly in the eastern half of the city. In the east-northeastern and western parts of the city, there are three similar neighborhoods built as compact areas of residential buildings with ten floors or more, designed to sustain the massive urbanization campaign launched by the communist regime (E, G, and I in Fig. 1). The influence of the mountain breeze, dominant in the western and southwestern areas of the city during the night and morning, combined in the daytime with the small-scale advection towards the city of cooler air from the forest area, located at the southwestern limit of the city, moving the warm air from

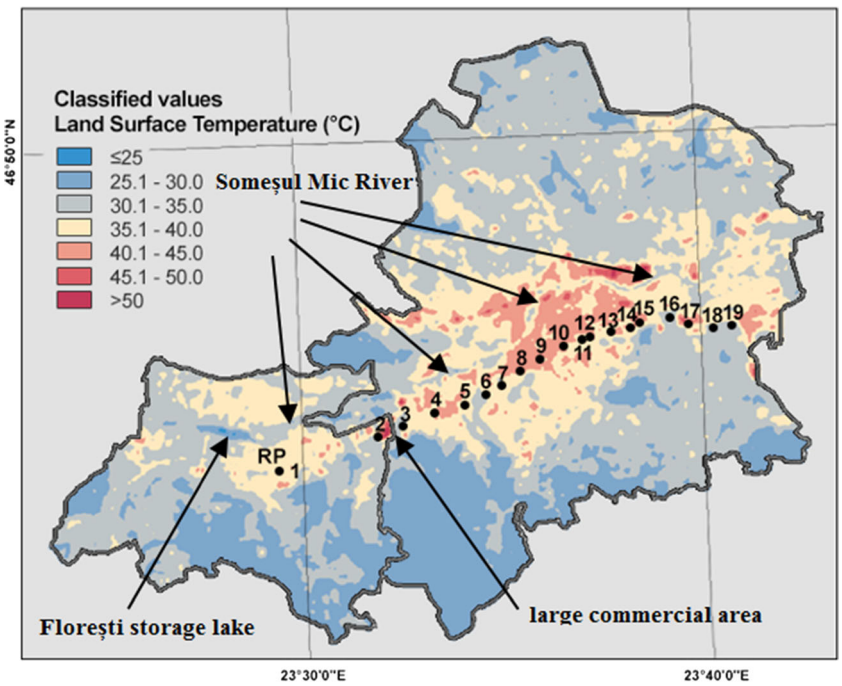

Fig. 4 Cluj-Napoca SUHI detected based on Landsat imagery on July 7, 2015

Table 3 LST by classes for the three case studies

LST class	Area (%)		
	July 7	July 23	August 8
<25	0.01	0.08	0.18
25.1…30	22.57	19.26	19.78
30.1…35	48.44	44.33	33.60
35.1…40	23.60	31.99	41.20
40.1…45	5.03	4.12	5.11
45.1…50	0.32	0.20	0.13
>50	0.03	0.02	0.00
Total area	100.00	100.00	100.00

Mănăștur neighborhood (I area) eastward and replacing it with the cooler one, on the thermal map, the warmest was the east-northeastern one (Fig. 5). Under these circumstances, we can conclude that, at least before noon, similar urban tissue can have different behavior in the urban area under the impact of local air circulation.

3.2 Surface urban heat island extension and intensity on July 23, 2015

The synoptic map of July 23, 2015 indicates, at 00:00 UTC, the activity of a weak high-pressure mobile system over the Black Sea (1015–1020 hPa), developed under a high ridge extended from Northern Africa, while 12 h later, its extension diminished significantly till the extinction and a few low-pressure mobile systems occurred over the whole area which registered a decrease in SLP (1010–1015 hPa) (Fig. 6). The sea level pressure (SLP) was slightly above normal, with values up to 1018 hPa. July 23 was the first day of a severe HW event, generated by the advection of warm air mass from a northward branch of the high-altitude ridge. The association of the high-pressure system with the North-African air mass induced a 4-day lasting HW from July 22 to July 25. The first day was of moderate intensity, while the next 3 days are included in the category of severe HW.

Favorable weather conditions were also encountered at noon on July 23, when the satellite passed over the study area. When the satellite image was captured, the area of interest was cloud free, but a cloud system of cumulus and cumulonimbus developed few hours later over the eastern part of the city area, indicating a strong atmospheric convection due to the intense warming of the city surface. As a result, a thunderstorm developed later in that evening.

On July 23, the LST map showed a stronger SUHI compared to the first study case, in terms of mean temperature over the city (33.5 °C) (Figs. 5 and 7). A detailed analysis of the surface, covered by different temperature classes (Table 3), indicates that only the class between 35 and 40 °C increased in area compared to the previous study case, while all the other classes above 25 °C diminished their area. The largest area of the city recorded LST in the range of 30.1–35.0 °C, while the LST class of 35.1–45.0 °C covered more than 35% of the entire region under study (Table 3). The surface temperature patterns were, nevertheless, very similar with the previous one. The minimum temperature was recorded over Florești water storage reservoir (20.6 °C), and the highest temperatures were distributed in the built-up area and over land with low-vegetation coverage. The large hot-spots corresponded to industrial areas with values up to 51.7 °C (on a steel rooftop of a factory), followed by the Old City area. The rooftop of the commercial area in the western part of the city and the large parking in front of it induced values ranging from 45.1 to 50.0 °C, while temperatures above 40.0 °C were recorded in the central part of the city and in the eastern concrete and asphalt dominated neighborhood (Fig. 7).

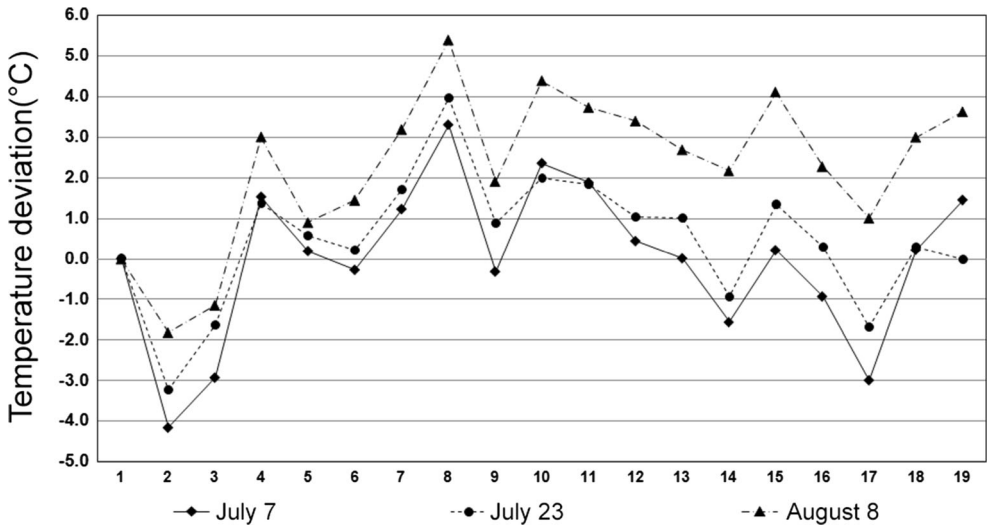

Fig. 5 Deviation of the LST in the pixels of the transects from the reference point LST

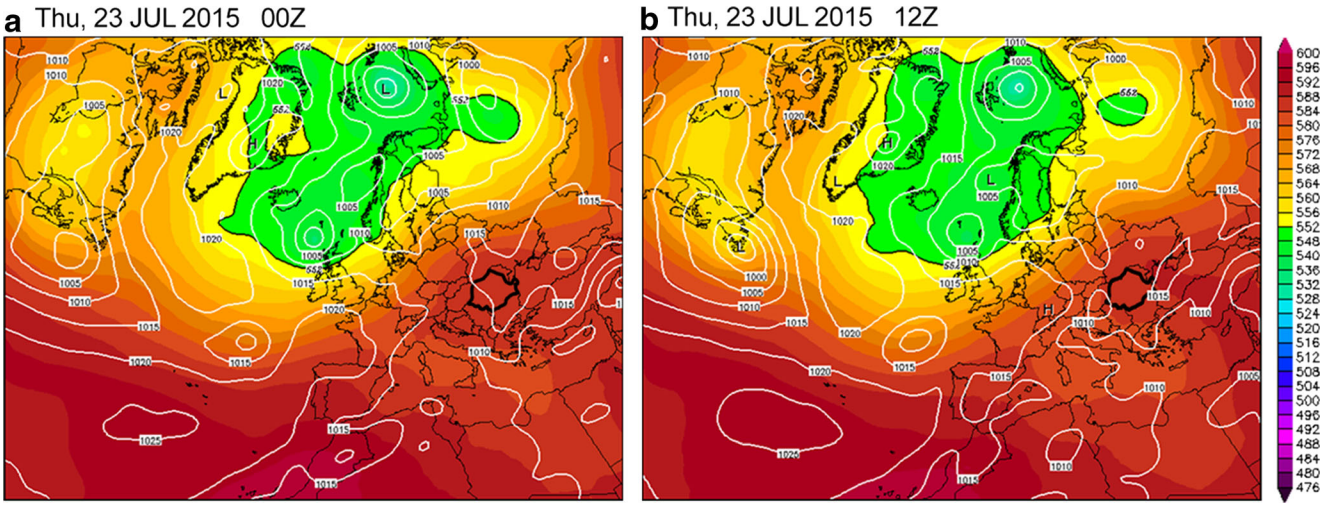

Fig. 6 Synoptic conditions on July 23, 2015 (source www.wetterzentrale.de, modified): at 00:00 UTC (**a**) and at 12:00 UTC (**b**). The Romania's territory is emphasized in black thick line)

3.3 Surface urban heat island extension and intensity on August 8, 2015

The synoptic maps valid for the 8th of August indicated a southern warm advection through a mobile high-pressure system (1020–1025 hPa) generated by the extension of a North African High over Eastern Europe (Fig. 8). At 500 hPa level, there was an advection of tropical air mass in a warm high-altitude ridge (more than 580 damg) also originated in Northern Africa. This situation favored the occurrence of one of the longest, most severe HWs ever registered in Cluj-Napoca, which started on August 4 and ended in August 16 (13 days). During that event, there were two episodes of extremely severe HW: August 5–8 and August 10–15 (Table 2). It was the most intense HW among all the three case studies. No clouds covered the city area at the moment of the satellite image capture, but the convective clouds that occurred few hours later in the same day indicated the presence of a strong thermal convection. Even though the absolute air temperature values during the satellite passage was lower compared to the ones registered in the previous situations, the average LST for the entire area was higher compared to the previous case studies (34.0 °C). The area with values above 40.0 °C was the largest among all the situations considered for this paper (more than 5%), and it was identified over the industrial regions in the eastern part of the city, in the city

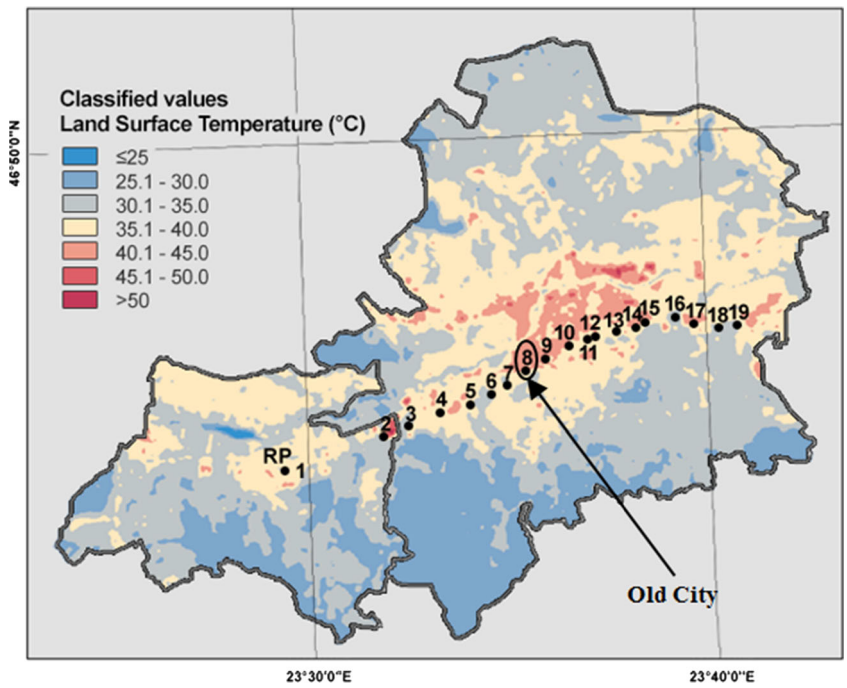

Fig. 7 Cluj-Napoca SUHI detected based on Landsat image on July 23, 2015

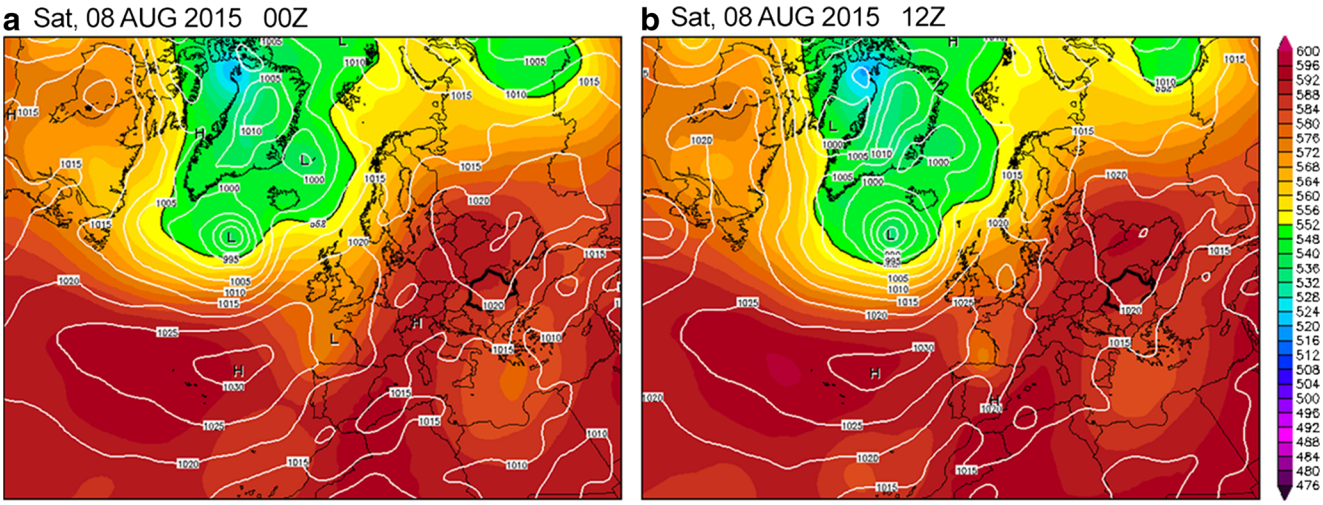

Fig. 8 Synoptic conditions on August 8, 2015 (source www.wetterzentrale.de, modified): at 00:00 UTC (**a**) and at 12:00 UTC (**b**). The Romania's territory is emphasized in black thick line)

center, and the compact residential neighborhoods (Fig. 9). The area affected by high temperatures ranging from 35 to 40 °C (more than 41%) was also the largest of the three cases (Table 3), and its extension was generated not only by urban built area but also by the agriculture land use with less dense vegetation, depending on the crop type and harvesting period. There are some similarities with LST spatial distribution during the other HW events: the lowest temperature was recorded by Floreşti water storage reservoir (19.6 °C) and the highest over the commercial area in the western part of the city (50.4 °C) (Fig. 9). The highest intensity among all the three situations analyzed in this paper can be observed also on the LST deviation calculated on the transect points (Fig. 5).

3.4 The impact of HWs on the surface urban heat island intensity

In order to detect how much HW events influenced the intensity of SUHI, we extracted the LST values for 18 sample pixels (except the RP) located on a transect crossing the city from west to east, along the main traffic road of the city from all satellite images available and valid for further processing (Fig. 10). We grouped the satellite images in three sub-groups based on the date of the image capture and in each of them there were included images got in the same day of the calendar or around that day but in different years.

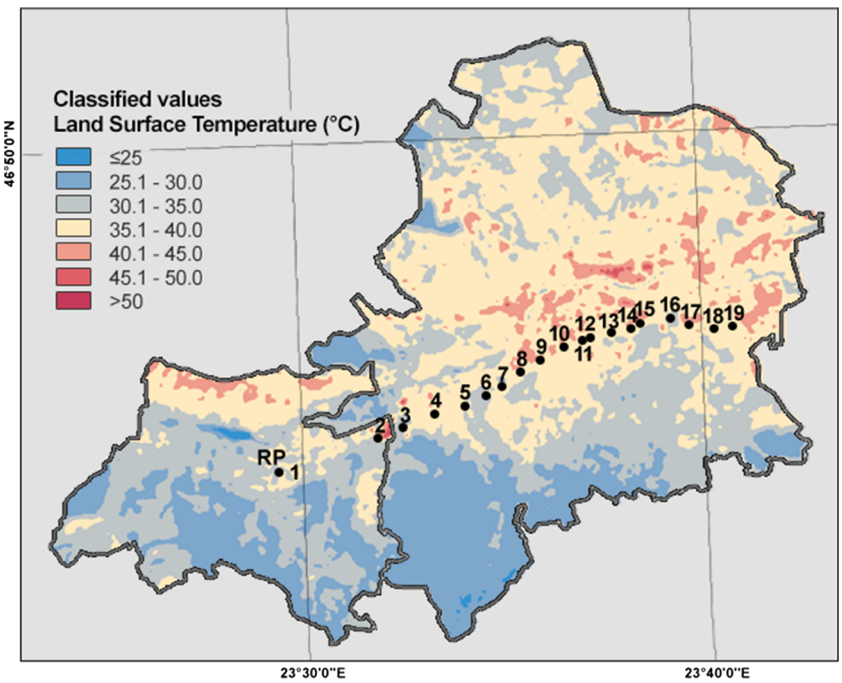

Fig. 9 Cluj-Napoca SUHI detected based on Landsat image on August 8, 2015

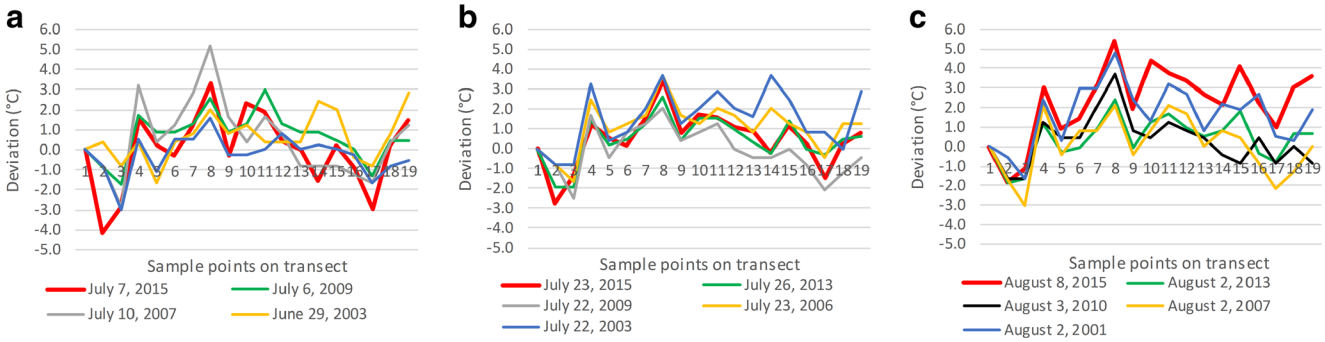

Fig. 10 Deviation of LST from RP calculated for the sample points along the West-East transect: at the beginning of July (**a**), at the end of July (**b**), and at the biginning of August (**c**)

The results revealed that even though we focused our points "on the road," there were some important differences from the RP, rising up to 5 °C along the transect (Fig. 10). The difference among the deviation values of different points (pixels) was caused by the specific surface of each pixel (e.g., points 2 and 3 versus points 8, 10, and 11). The 30 m resolution pixels usually include the street, the sidewalk, and sometimes vegetation or buildings. When vegetation is included in the pixel or in the nearby pixels, the surface temperature detected was much lower, as in the case of points 2 or 3 (Fig. 10), which recorded usually negative deviations, while in high-density built-up areas, the temperature detected increased compared to the RP and those points constantly experienced the highest positive deviations (points 6–13).

The analysis of the surface temperature deviation of the 18 sample points, performed for all available satellite images, indicated that the SUHI intensity increased with the intensity of the HW, and seemed to be influenced only by extremely severe HWs. Thus, in case of the last HW event analyzed, the deviation values from RP LST were the highest, exceeding 5.0 °C in the city center (represented by point 8). Other peaks were located in the concrete high-buildings neighborhood (points 10 and 11), and in the outside parking of a large hypermarket (point 4). The LST pattern remained the same for all the situations considered, but the intensity was different from one situation to another. During the third HW event considered for this study (Fig. 10c), which was classified as extremely severe, the deviation values from the RP were the highest compared to all the other non-HW situations in some of the points, while SUHI intensity does not differ during the first two HW events, classified as severe (satellite images captures on July 7 and July 23, 2015), compared to the other non-HW situations (Fig. 10a, b). The deviations recorded during the first two HWs are around the average values among all the values detected. Under this circumstances, we can state that, based on the available data, only extremely severe HWs seems to slightly increase the intensity of SUHI, while severe (and most likely, also moderate) ones do not intensify the SUHI. But, due to the low number of satellite image available, we have to be cautious with this conclusion.

3.5 Impact of the heat waves on the work productivity and local economy

The effects of very high temperature are extremely important leading to loss of productivity, health problems, or even life threatening. Although more research is needed in order to accurately compare the costs of taking action to the potential loss of productivity, the existing results already indicate that the latter are significantly higher than the former, maybe even with an order of magnitude.

For this analysis we used the number of employees in Cluj-Napoca city (90,000) and an hourly productivity of 11.8 EUR/person/h, obtained from adjusting the Romanian average of 5.6 EUR/person/h to match the workforce structure in Cluj-Napoca. Finally, we got an estimated potential loss of productivity of 2,548,000 EUR/day, and in case of considering all the 15 HW days during the work week, the loss increased to more than 38.2 mil. EUR. Even though we excluded the weekend days from this study, they could have had an important impact, especially in those situations when the people did not leave the city over the weekend and their houses did not have air conditioned devices. Moreover, if we consider the impact of the UHI and assume a longer duration of the HWs in the urban areas compared to the standard weather stations conditions, we could obtain even higher values of economic loss generated by heat stress.

The Romanian legislation stipulates several minimal measures that have to be provided by the employers during periods of increased temperatures, including decreased work intensity, alternating work with rest periods, in shaded and ventilated areas and providing the employees with ventilation and with adequate water supplies (2–4 l per person). In the cases when these conditions cannot be met, the employees can decide to reduce the work period, to split it into two separate periods (until 11:00 a.m. and after 5:00 p.m.), or to even collectively suspend work. However, all these measures come into force only in extreme conditions, when the temperature is 37.0 °C or higher for at least two consecutive days in standard weather station conditions, so they do not apply when an HW starts from below that temperature (OU 99/2000 2000), even though the heat stress increases in urban areas due to UHI.

4 Conclusions

The present study investigated the LST patterns during three HW events (two severe and one extremely severe) that affected Cluj-Napoca area during the summer of 2015 using Landsat 8 satellite image data, as well as the economic loss generated by the occurrence of these three events.

The main limitation of this study is that the results should be considered as preliminary due to the low number of satellite images available. Further analysis should be performed in the next years when more satellite images will be available or based on direct measurements in case that an urban climate monitoring system will be installed.

However, Landsat 8 imagery has proven to be a very useful tool for SUHI evaluation as it provides the means to compute the LST of mid-extension cities. In such areas, the temperature retrieved by low-resolution sensors with higher revisiting time such as MODIS is rather questionable because of the spatial averaging of the heterogeneous urban fabric.

Overall, the SUHI has been detected on all situations considered, with LST values exceeding by 5.0 °C, the RP LST. As expected, the lowest temperature values were detected over the land covered by forest, green areas, and water, and the highest in industrial and commercial areas, in the city center, and in the neighborhoods with compact residential high-density and elevation buildings.

However, even though similar urban fabric is specific in the eastern and western part of the city, the SUHI detected for Cluj-Napoca is asymmetrical and more intense in the eastern half of the city for all analyzed HW events. The local mountain breeze, which is dominant in the western and southwestern areas of the city during the night and morning, combined in the daytime with the small-scale advection towards the city of cooler air from the forest area (located at the southwestern limit of the city), moving the warm air eastward from western neighborhoods toward the eastern ones, seem to be the main factors generating the SUHI asymmetry, detected around noon based on LST derived from satellite images.

For the entire area considered, the shape of the SUHI remained almost the same, but intensity seems to have been influenced by the magnitude of the HW event. We found that only when an extremely severe HW occurred, a weak intensification of the SUHI has been recorded, especially in the central and eastern part of the city, while during severe HW events, intensity of SUHI seemed to be similar to that recorded under no heat waves conditions. Also, during the extremely severe HW, due to the intense warming of agricultural land, the SUHI became larger and covered also the agricultural area without vegetation around the city built-up area. However, due to the low number of satellite images available, we have to be cautious with this conclusion and consider this study as presenting preliminary results, while the same type of analysis should be performed in the upcoming years, based on a higher number of study cases.

The economic loss estimated for Cluj-Napoca urban area under HW conditions (amplified by UHI) can reach about 2.5 mil. EUR/day in the summer (totaling more than 38.2 mil. EUR for all HW events considered for this study), and this could imply important negative consequences for the whole community. This result should not be expanded at regional or national level, since it is calculated specifically for Cluj-Napoca city, but the methodology can be used in order to estimate the potential loss for other big cities. For each city, it should take into account the number of employees, workforce structure, and office equipment, if possible, at least, from the perspective of air conditioned use where/if the data is available. In order to conduct such a study on larger area, calculation of potential loss should be performed for as much as possible cities in the area considered and after that it can be aggregated at regional/national level. Such evaluation reports can become useful tools for local, regional, and national planning and development strategies. The HWs, as demonstrated, could have a significant effect on a city productivity and, consequently, on its budget and development, but the evaluation and the needed actions have to be performed and decided by each city authority, based on its own characteristics.

This study could be extremely important for local and national authorities in order to improve the early warning systems for HWs based on implementation of a new infrastructure for UHI monitoring and on developing specific thresholds for small-scale (urban area) weather forecast. The warning thresholds established by the National Meteorological Administration can be easily exceeded in urban areas while in the standard weather stations, the temperature is below the thresholds. These measures are necessary for big cities in order to get data from inside urban area for a more objective analysis (Larsen 2015; Cao et al. 2015; Hoelscher et al. 2016). This kind of analysis would help managers and policy makers to adopt the most appropriate measures in order to mitigate the impact of heat stress in big cities generated by HWs and amplified by UHI.

Acknowledgements This research was developed under the framework of the project *Extreme weather events related to air temperature and precipitation in Romania*, project code PN-II-RU-TE-2014-4-0736, funded by the Executive Unit for Financing Higher Education, Research, Development, and Innovation (UEFISCDI) in Romania. The work was also partially supported by the *Sectorial Operational Program for Human Resources Development 2007-2013*, co-financed by the *European Social Fund*, under the project number POSDRU/159/1.5/S/132400 titled *Young successful researchers—professional development in an international and interdisciplinary environment.* The authors acknowledge the USGS for freely provided LANDSAT 8 imagery, the reliable prognosis 5 days for weather data for Cluj-Napoca weather station, the National Bank of Romania, the National Institute of Statistics, and Eurostat for freely provided economic data. The authors bring kind acknowledgements to the three anonymous reviewers for their useful comments and suggestions, which helped us to improve the quality of this paper.

References

Apostol L, Alexe C, Sfică L (2012) Thermic differentiations in the Iaşi municipality during a heat wave. Case Study July 10–20 2011. Present Environ Sustain Dev 1:395–404. Atmospheric Correction Parameter Calculator, URL http://atmcorr.gsfc.nasa.gov/. Accessed 8 May 2016

Barsi JA, Schott JR, Palluconi FD, Hook SJ (2005) Validation of a web-based atmospheric correction tool for single thermal band instruments. In: Proc. SPIE 5882, Earth Observing Systems X, 58820E. p 58820E–58820E–7. doi:10.1117/12.619990

Basara JB, Basara HG, Illston BG, Crawford KC (2010) The impact of the urban Heat Island during an intense heat wave in Oklahoma City. Adv Meteorol 2010:1–10. doi:10.1155/2010/230365

Ben-Dor E, Saaroni H (1997) Airborne video thermal radiometry as a tool for monitoring microscale structures of the urban heat island. Int J Remote Sens 18:3039–3053. doi:10.1080/014311697217198

Bottyan ZS, Kircsi A, Szegedi S, Unger J (2005) The relationship between built-up areas and the spatial development of the mean maximum urban heat island on Debrecen, Hungary. Int J Climatol 25: 405–418. doi:10.1002/joc.1138

Campetella C, Rusticucci M (1998) Synoptic analysis of an extreme heat wave over Argentina in March 1980. Met Apps 5:217–226. doi:10.1017/S1350482798000851

Cao MC, Rosado P, Lin ZH, Levinson R, Millstein D (2015) Cool roofs in Guangzhou, China: outdoor air temperature reductions during heat waves and typical summer conditions. Environ Sci Technol 49(24):14672–14679. doi:10.1021/acs.est.5b04886

Carlson TN, Ripley DA (1997) On the relation between NDVI, fractional vegetation cover, and leaf area index. Remote Sens Environ 62:241–252. doi:10.1016/S0034-4257(97)00104-1

Chander G, Markham B (2003) Revised Landsat-5 TM radiometric calibration procedures and postcalibration dynamic ranges. IEEE Trans Geosci Remote Sens 41:2674–2677. doi:10.1109/TGRS.2003.818464

Cheval S, Dumitrescu A (2015) The summer surface urban heat island of Bucharest (Romania) retrieved from MODIS images. Theor Appl Climatol 121:631–640. doi:10.1007/s00704-014-1250-8

Cheval S, Dumitrescu A (2009) The July urban heat island of Bucharest as derived from modis images. Theor Appl Climatol 96:145–153. doi:10.1007/s00704-008-0019-3

Cheval S, Dumitrescu A, Bell A (2009) The urban heat island of Bucharest during the extreme high temperatures of July 2007. Theor Appl Climatol 97:391–401. doi:10.1007/s00704-008-0088-3

Costa H, Floater G, Hooyberghs H, Verbeke S, De Ridder K (2016) Climate change, heat stress and labour productivity: a cost methodology for city economies, Centre for Climate Change Economics and Policy Working Paper No. 278 Grantham Research Institute on Climate Change and the Environment Working Paper No. 248. Available at: http://www.lse.ac.uk/GranthamInstitute/wp-content/uploads/2016/07/Working-Paper-248-Costa-et-al.pdf. Accessed 8 Oct 2016

Croitoru AE, Antonie RI, Rus A (2014) Heat waves and their estimated socio-economic impact in Bucharest City, Romania. Proceedings of the International Multidisciplinary Scientific GeoConference-SGEM. Book Group Author(s):SGEM GEOCONFERENCE ON ENERGY AND CLEAN TECHNOLOGIES, VOL II. Book Series: International Multidisciplinary Scientific GeoConference-SGEM: 375–382. doi:10.5593/sgem2014B41. Available at: http://connection.ebscohost.com/c/articles/101013777/heat-waves-their-estimated-socio-economic-impact-bucharest-city-romania. Accessed 7 Aug 2016

Ćurić M (2012) Measuring system of adverse weather phenomena. Proceedings of the International Conference Air and Water Components of the Environment: 68–73. Available at: http://aerapa.conference.ubbcluj.ro/2012/pdf/09%20Curic%20.pdf. Accessed 5 Aug 2016

Department of the Interior U.S. Geological Survey (2016) Landsat 8 data users handbook V 2.0. EROS: Sioux Falls, South Dakota. Available at: https://landsat.usgs.gov/sites/default/files/documents/Landsat8DataUsersHandbook.pdf. Accessed 5 Sept 2016

Dousset B, Gourmelon F, Laaidi K, Zeghnoun A, Giraudet E, Bretin P, Maurid E, Vandentorren S (2011) Satellite monitoring of summer heat waves in the Paris metropolitan area. Int J Climatol 31:313–323. doi:10.1002/joc.2222

European Community (2015) Eurostat platform. Available at: http://ec.europa.eu/eurostat/web/products-datasets/-/tsdec310. Accessed 8 Aug 2016

Founda D, Pierros F, Petrakis M, Zerefos C (2015) Interdecadal variations and trends of the urban heat island in Athens (Greece) and its response to heat waves. Atmos Res 161–162:1–13. doi:10.1016/j.atmosres.2015.03.016

Gabriel KMA, Endlicher WR (2011) Urban and rural mortality rates during heat waves in Berlin and Brandenburg, Germany. Environ Pollut 159:2044–2050. doi:10.1016/j.envpol.2011.01.016

Gallo KP, McNab AL, Karl TR et al (1993) The use of NOAA AVHRR data for assessment of the urban heat island effect. J Appl Meteorol 32:899–908. doi:10.1175/1520-0450(1993)032<0899:TUONAD>2.0.CO;2

Hoelscher MT, Nehls T, Janicke B, Wessolek G (2016) Quantifying cooling effects of facade greening: shading, transpiration and insulation. Energ Buildings 114(Special Issue):283–290. doi:10.1016/j.enbuild.2015.06.047

Hu LQ, Monaghan AJ, Brunsell NA (2015) Investigation of urban air temperature and humidity patterns during extreme heat conditions using satellite-derived data. J Appl Meteorol Climatol 54(11):2245–2259. doi:10.1175/JAMC-D-15-0051

Hu Y, Jia G (2009) Influence of land use change on urban heat island derived from multi-sensor data. Int J Climatol 30:1382–1395. doi:10.1002/joc.1984

Icaza LE, Van den Dobbelsteen A, Van der Hoeven F (2016) Surface thermal analysis of North Brabant cities and neighbourhoods during heat waves. TEMA-J Land Use Mobil Environ 9(1):66–90. doi:10.6092/1970-9870/3741

Jiménez-Muñoz JC, Sobrino JA, Skoković D et al (2014) Land surface temperature retrieval methods from Landsat-8 thermal infrared sensor data. IEEE Geosci Remote Sens Lett 11:1840–1843. doi:10.1109/LGRS.2014.2312032

Kawashima S, Ishida T, Minomura M, Miwa T (2000) Relations between surface temperature and air temperature on a local scale during winter nights. J Appl Meteorol 39:1570–1579. doi:10.1175/1520-0450(2000)039<1570:RBSTAA>2.0.CO;2

Klein Tank AMG et al (2002) Daily dataset of 20th-century surface air temperature and precipitation series for the European climate assessment. Int J Climatol 22:1441–1453. doi:10.1002/joc.773

Laaidi K, Zeghnoun A, Dousset B et al (2012) The impact of Heat Islands on mortality in Paris during the August 2003 heat wave. Environ Health Perspect 120:254–259. doi:10.1289/ehp.1103532

Larsen L (2015) Urban climate and adaptation strategies. Front Ecol Environ 13(9):486–492. doi:10.1890/150103

Li D, Bou-Zeid E (2013) Synergistic interactions between urban heat islands and heat waves: the impact in cities is larger than the sum of its parts. J Appl Meteorol Climatol 52:2051–2064. doi:10.1175/JAMC-D-13-02.1

McKinnon M, Buckle E, Gueye K, Toroitich I, Ionesco D, Mach E, Maiero M (eds) (2016) Kjellstrom T, Otto M, Lemke B, Hyatt O, Briggs D, Freyberg C, Lines L (Technical authors). Climate change and labour: impacts of heat in the workplace, climate change, workplace and environmental conditions, occupational, health risks, and productivity—an emerging global challenge to decent works, sustainable development and social equity. International Labour

Organization. Available at: http://www.ilo.org/wcmsp5/groups/public/—ed_emp/—gjp/documents/publication/wcms_476194.pdf. Accessed 1 Nov 2016

Meteomanz (2016) Archive of SYNOP/BUFR observations. Data by days. Available at: http://www.meteomanz.com. Accessed 30 Aug 2016

National Bank of Romania (2015a) Monthly bulletin July 2015, XXIII, 261. Available at: http://www.bnr.ro/Regular-publications-2504.aspx.e2015bl07.pdf. Accessed 15 Nov 2016

National Bank of Romania (2015b) Monthly bulletin August 2015, XXIII, 262. Available at: http://www.bnr.ro/Regular-publications-2504.aspx.e2015bl08.pdf. Accessed 15 Nov 2016

Nichol JE, Fung WY, Lam K, Wong MS (2009) Urban heat island diagnosis using ASTER satellite images and "in situ" air temperature. Atmos Res 94:276–284. doi:10.1016/j.atmosres.2009.06.011

OU 99 (2000) Ordonanta de urgenta nr. 99/2000 din 29/06/2000, privind masurile ce pot fi aplicate in perioadele cu temperaturi extreme pentru protectia persoanelor incadrate in munca. Monitorul Oficial 304/4 iulie 2000. Available at: https://www.iprotectiamuncii.ro/legi/oug-99-2000.pdf. Accessed 30 Sept 2016

Parsons K (2009) Maintaining health, comfort and productivity in heat wave global health action. Glob Health Action 2. doi:10.3402/gha.v2i0.2057

Pogacar T, Zalar M, Crepinsek Z, Bogataj K, Ciuha U, Mekjavic I (2016) Impact of heat waves on labour productivity—case study for industry, EMS annual meeting abstracts vol. 13, EMS2016-510, 2016 16th EMS / 11th ECAC © Author(s) 2016. CC Attribution 3.0 License. EMS Annual Meeting European Conference on Applied Climatology ECAC

Prihodko L, Goward SN (1997) Estimation of air temperature from remotely sensed surface observations. Remote Sens Environ 60:335–346. doi:10.1016/S0034-4257(96)00216-7

Radinovic D, Curic M (2013) Measuring system of adverse weather phenomena. (Abstract). Disaster Adv 6(3):19–23

Reliable Prognosis (2016) Weather archive in Cluj-Napoca. Available at: https://rp5.ru/Weather_archive_in_Cluj-Napoca. Accessed 19 Aug 2016

Robine J-M, Cheung SLK, Le Roy S et al (2008) Death toll exceeded 70,000 in Europe during the summer of 2003. Comptes Rendus Biologies 331:171–178. doi:10.1016/j.crvi.2007.12.001

Roth M, Oke TR, Emery WJ (1989) Satellite-derived urban heat islands from three coastal cities and the utilization of such data in urban climatology—International Journal of Remote Sensing—Volume 10, Issue 11. Int J Remote Sens 10:1699–1720

Sfică L, Croitoru AE, Iordache I, Ciupertea AF (2017) Synoptic conditions generating heat waves and warm spells in Romania. Atmosphere 8:50. doi:10.3390/atmos8030050

Sobrino JA, Jimenez-Munoz JC, Paolini L (2004) Land surface temperature retrieval from LANDSAT TM 5. Remote Sens Environ 90:434–440

Stewart ID (2011) A systematic review and scientific critique of methodology in modern urban heat island literature. Int J Climatol 31:200–217. doi:10.1002/joc.2141

Stoll MJ, Brazel AJ (1992) Surface-air temperature relationships in the urban environment of phoenix, Arizona. Phys Geogr 13:160–179. doi:10.1080/02723646.1992.10642451

Tan J, Zheng Y, Tang X et al (2010) The urban heat island and its impact on heat waves and human health in Shanghai. Int J Biometeorol 54:75–84. doi:10.1007/s00484-009-0256-x

Unger J, Gál T, Rakonczai J, Mucsi L, Szatmári J, Tobak Z, van Leeuwen B, Fiala K (2010) Modeling of the urban heat island pattern based on the relationship between surface and air temperatures. Időjárás 114:287–302

Unger J, Savic SM, Gál T, Milosevic DD (2014) Urban climate and monitoring network system in European cities. University of Novi Sad, Faculty of Sciences (UNSPMF) and University of Szeged, Department of Climatology and Landscape Ecology (SZTE), Novi-Sad (Serbia)—Szeged (Hungary)

USGS (2016) EarthExplore. Available at: http://earthexplorer.usgs.gov. Accessed 8 May 2016

Ward K, Lauf S, Kleinschmit B, Endlicher W (2016) Heat waves and urban heat islands in Europe: a review of relevant drivers. Sci Total Environ 569:527–539. doi:10.1016/j.scitotenv.2016.06.119

Weng Q, Lu D, Schubring J (2004) Estimation of land surface temperature–vegetation abundance relationship for urban heat island studies. Remote Sens Environ 89:467–483. doi:10.1016/j.rse.2003.11.005

Wetterzentrale (2016) Archiv. Reanalyse. Available at: http://www.wetterzentrale.de. Accessed 5 Aug 2016

Xiong Y, Huang S, Chen F et al (2012) The impacts of rapid urbanization on the thermal environment: a remote sensing study of Guangzhou, South China. Remote Sens 4:2033–2056. doi:10.3390/rs4072033

Yuan F, Bauer ME (2007) Comparison of impervious surface area and normalized difference vegetation index as indicators of surface urban heat island effects in Landsat imagery. Remote Sens Environ 106:375–386. doi:10.1016/j.rse.2006.09.003

Zander KK, Botzen WJW, Oppermann E, Kjellstrom T, Garnett ST (2015) Heat stress causes substantial labour productivity loss in Australia. Nat Clim Chang 5:647–651. doi:10.1038/nclimate2623

Zhou Y, Shepherd JM (2010) Atlanta's urban heat island under extreme heat conditions and potential mitigation strategies. Nat Hazards 52:639–668. doi:10.1007/s11069-009-9406-z